ELSEVIER

Thermochimica Acta 300 (1997) 127–139

thermochimica acta

The oxidation of sulphide minerals

J.G. Dunn*

A.J. Parker Cooperative Research Centre for Hydrometallurgy, School of Applied Chemistry, Curtin University of Technology, PO Box U1987 Perth WA 6001, Australia

Received 25 July 1996; received in revised form 8 August 1996; accepted 20 November 1996

Abstract

The literature associated with the thermal behaviour of mineral sulphides has been selectively and critically reviewed. Particular attention has been paid to:

- the importance of characterising the starting material, as well as intermediate products
- the effect of experimental variables on the thermal analysis results

The various reactions that sulphides can undergo in inert and oxidising atmospheres are presented. Under mild oxidising conditions, such as an air atmosphere and heating rates of 10–20°C min^{-1}, the oxidation occurs as a sequence of reactions usually controlled by oxygen diffusion, although in some situations decomposition of the sulphide with evolution of sulphur can occur. Besides the formation of oxides and sulphates, and the subsequent decomposition of the latter, solid–solid reactions can occur between sulphates and unreacted sulphides. In ternary systems, such as the iron-nickel sulphides, considerable ion diffusion can take place.

Under more vigorous oxidising conditions, such as an oxygen atmosphere with a heating rate in excess of 40°C min^{-1}, some sulphides can be ignited. Under these conditions the relative ignition temperatures of sulphides can be measured, and the effects of variables such as particle size and stoichiometry on the ignition temperature examined.

The oxidation of pyrite is presented as a case study of the effects of experimental variables on the results of thermal analysis. The application of the results of studies to the industrial processing of sulphides of economic importance has been discussed. © 1997 Elsevier Science B.V.

Keywords: Characterisation; Ignition; Oxidation; Pyrolysis; Sulphide minerals

1. Introduction

One of the major industries in Western Australia comprises mining and mineral processing, which earns about $12 billion per annum in export income. Although many of the minerals processed are oxides, such as iron ore deposits of hematite and goethite, there are also many sulphide minerals of economic importance. These may be important as the primary source of a metal, such as the nickel deposits, or as the host matrix for gold, as in the case of gold-bearing arsenopyrite and pyrite deposits. Since one of the major processing routes for sulphides is thermal

*Corresponding author. Fax: 619-3512300; e-mail: J.Dunn@cc.curtin.edu.au.

PII S0040-6031(96)03132-2

conversion to a matte or oxide, by smelting or roasting, it seemed appropriate to use thermal methods of analysis to study these reactions.

Sulphides are amenable to study by thermal methods of analysis, as they undergo a variety of reactions which cause mass and energy changes. There are many examples of such studies in the literature, although it is apparent that there are significant differences in the results and interpretation of results on studies purported to be on the same mineral. These variations range from a difference in the number of thermal events which have been observed in particular thermal analysis experiments, the temperature ranges within which these events occurred, and the assignment of reactions to these events. Hence, although the final products of the reactions were usually reported to be the same, the reaction path and the associated thermal events are frequently different. Most of these problems arise from two major sources:

- Insufficient characterisation of the starting compound, especially for natural minerals which frequently contain significant levels of impurities. Intermediate products were often not well characterised either, so that some of the thermal events were assigned to reactions on a speculative rather than proven basis.
- In attention to the importance of experimental variables, such as heating rate and atmosphere, on the reaction sequence. These variables have long been known to affect the results obtained, and have been discussed comprehensively in recent texts [1,2].

2. Characterisation of the sample

Some 25 years ago, characterisation of the sample was limited to chemical analysis and X-ray diffraction, and these two measurements would be regarded as the very minimum requirements for characterisation purposes. These were, however, bulk characterisation methods. Since then, a whole new range of methods has arrived on the scene which are able to provide information on the properties of individual particles. The earliest examples of these are scanning electron microscopy (SEM) and electron probe microanalysis (EPMA), which can not only provide visual images of the particles but also the qualitative and quantitative information about element distribution in the particles. These techniques have been augmented by others such as Auger spectroscopy, etc. By mounting the particles in an epoxy resin and polishing the surface, the internal structure of the particle may be revealed and analysed. The techniques can be used to determine impurities, as well as to check homogeneity of composition within a particle.

Another technique which has enjoyed a renaissance is Fourier transform infrared (FTIR) spectroscopy, which has much improved sensitivity and resolution relative to infrared spectroscopy. Examination of both starting material and reacted products, in the form of a KBr disc or by diffuse reflectance, provides a sensitive means of again determining, qualitatively and quantitatively, minor phases such as sulphates and arsenates, which are often difficult to detect by XRD. FTIR has the added advantage that it can often differentiate between the different oxidation states of a compound. For example, the FTIR spectrum of $FeSO_4$ is quite different to that of $Fe_2(SO_4)_3$ [3].

The arsenal of characterisation techniques available to the thermal analyst enables chemical reactions to be assigned to thermal events with confidence.

3. Thermal reactions of sulphides

Studies on the thermal behaviour of sulphides are generally carried out under three sets of conditions:

- *under an inert atmosphere*, so that the pyrolysis behaviour of the sulphide is followed;
- *under mild oxidising conditions*, so that the sulphide is oxidised in a step-wise reaction sequence with the production of various intermediates, some of which may react at higher temperatures; and
- *under vigorous oxidising conditions*, so that the sulphide is ignited.

The results of experiments carried out under the second and third sets of conditions can be used to derive the reaction scheme that occurs during the pyrometallurgical processing of sulphide minerals. Mild oxidising conditions are analogous to roasting operations, where the sulphide mineral undergoes a set of sequential reactions. Vigorous oxidising conditions are analogous to the flash smelting process, which is

classified as an ignition reaction. The reaction sequences and mechanisms of reaction can be found from information obtained from the phases present in the transition products.

3.1. Pyrolysis reactions of sulphides

Heating sulphides under an inert atmosphere, i.e. nitrogen or argon, can bring about two processes

- *Phase transformations, such as an $\alpha \leftrightarrow \beta$ phase transition.* Chalcocite (Cu_2S), for example, undergoes a change in crystal structure from rhombohedral to hexagonal between 100° and 120°C [4].
- *Conversion of one phase to another.* This may occur through decomposition of the sulphide to a more stable form, liberating gaseous sulphur. For example, covellite (CuS) has been reported to decompose to digenite in the 310° to 338°C range, with the liberation of sulphur [5]:

$$1.84CuS \rightarrow Cu_{1.84}S + 0.84S$$

Alternatively, the sulphide may be unstable and decompose with the formation of new phases. Fig. 1 shows the TG–DTA curve for a sample of pentlandite, $(Fe,Ni)_9S_8$. The first endotherm, which has no associated mass loss, indicates the decomposition at 610°C to produce two new phases, $(Fe,Ni)_{1-x}S$ and $(Fe,Ni)_{3+x}S_2$. The former is a solid solution of iron and nickel in a sulphur matrix, called mss, and the latter is heazlewoodite. Further heating causes the heazlewoodite to melt, as indicated by the second endotherm at 830°C. This then decomposes to produce solid mss and a liquid $(Fe,Ni)_{1+x}S_{1.0}$ with loss of sulphur, as indicated by the mass loss and the broad endotherm which commences at 845°C [6].

The extrapolated onset decomposition temperatures of some sulphides are given in Table 1 [7–9].

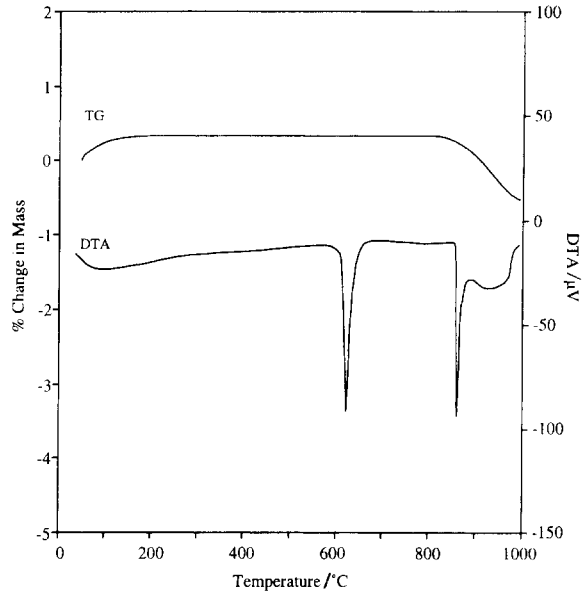

Fig. 1. Decomposition of pentlandite in nitrogen. Heating rate 20°C min^{-1}, particle size 45 to 63 μm [6].

3.2. Oxidation reactions of sulphides

The procedural variables, such as particle size, sample mass, heating rate, partial pressure of oxygen, and the size and composition of the sample pan, have an effect on the oxidation process of sulphides. Hence, these variables should be reported in any experimental work.

The increase in the temperature of a thermal event with increase in particle size, sample mass and heating rate is a well known effect, and is related to the thermal mass and conductivity of the sample [1,2].

The partial pressure of the oxidant can cause a change in the phases formed. This can be best illustrated by reference to predominance diagrams, first

Table 1
The onset decomposition temperatures of some metal sulphides

Formula	Mineral	Particle size in μm	Decomposition Temperature in °C	Reference
FeS_2	Pyrite	45–75	645	[7]
$Ni_{4.9}Fe_{4.45}S_8$	Pentlandite	45–75	610	[7]
$Ni_{2.0}Fe_{1.05}S_4$	Violarite	45–75	545	[7]
$Fe_{0.83}S$	Pyrrhotite, syn [a]	45–63	515	[8]
$Fe_{1.00}S$	Pyrrhotite, syn [a]	45–63	670	[8]
$CuFeS_2$	Chalcopyrite		800	[9]

[a] synthetically prepared.

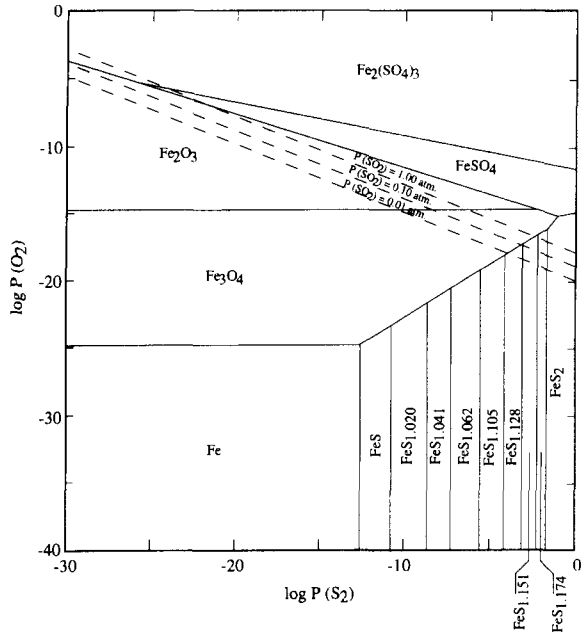

Fig. 2. Predominance diagram for the iron–sulphur system at 600°C.

proposed by Kellogg and Basu [10]. These diagrams plot the log of the oxygen partial pressure along one axis and the log of the sulphur partial pressure along the other. The predominance diagram for the iron–sulphur system is shown in Fig. 2. The bottom left-hand corner of the diagram is a region of low partial pressure of sulphur and oxygen, and is where the metal is the thermodynamically stable species. The left-hand axis shows an increase in oxygen partial pressure, and is the region where oxide species are stable. Sulphides are stable in high sulphur concentrations (bottom right-hand corner) and sulphates are stable in high concentrations of sulphur and oxygen (top right-hand corner). The dotted line indicates the partial pressure of sulphur dioxide, and the effect that changes in this value has on the phases present. The top line is for 1 bar of SO_2, the next line for 0.1 bar of SO_2, and the bottom line for 0.01 bar of SO_2. Under any of these partial pressures of SO_2, it is possible for Fe_3O_4 to co-exist with Fe_2O_3. If thermal experiments are carried out in open pans, with good gas exchange rates between the sample and the atmosphere, then the phases present will tend to be the higher oxidation states of iron, that is Fe_2O_3 and $Fe_2(SO_4)_3$. However, if the crucible is tall and narrow, such that gas exchange is inhibited and the atmosphere above the sample is oxygen deficient, then the phases present will tend to be the lower oxidation states of iron, that is Fe_3O_4, FeO, and $FeSO_4$. Thus, most reports identify Fe_2O_3 as a product of the oxidation of pyrite, but a few also identify Fe_3O_4 as a product [11,12], probably indicating that there has been an oxygen deficiency in the latter situation. It has also been demonstrated that the rate of oxidation of pyrite decreases by about one half as the wall height for the crucible increases from 2 to 4 mm [13].

Predominance diagrams are thus helpful in predicting the phases likely to be found during the oxidation process. The detection of certain phases will also assist in making some estimations about the gas composition above the sample.

Combinations of these variables can cause a complete change in the reaction mechanism, and produce TG–DTA traces which are totally different to one another. Some examples of such changes will be given later.

3.2.1. Oxidation under mild oxidising conditions

An examination of the studies carried out so far under mild oxidising conditions, which implies the use of air as the oxidant and a moderate heating rate of 10 to 20°C min^{-1}, indicates that the following types of reactions may be involved during the oxidation of sulphides.

3.2.1.1. Direct formation of oxide. The formation of oxide can be expressed in general as:

$$2MS_{(s)} + 3O_{2(g)} \rightarrow 2MO_{(s)} + 2SO_{2(g)}$$

The formation of SO_2 is highly exothermic, and consequently such reactions are readily detected as an exothermic peak in the DTA record. The conversion of sulphide to oxide produces a mass loss coincident with the exothermic event. The temperature at which oxidation of metal sulphides commences varies considerably, as indicated in Table 2 [12,14–23].

Oxide coatings can be quite protective, and inhibit the diffusion of oxygen to the unreacted sulphide. The temporary inhibition of the oxidation of inner material may favour other transformations. For example, further dynamic heating of the sample within the protective coating may produce decomposition of the sulphide. Since many of the sulphide minerals

Table 2
The onset oxidation temperatures of some metal sulphides

Formula	Mineral	Reaction temperature in °C	Reported product	Reference
FeS_2	Pyrite	400	FeS, S	[14]
		445	FeS, SO_2	[15]
		380	$Fe_{1-x}S$, SO_2	[16]
		500	$FeSO_4$, SO_2	[17]
		420	Fe_2O_3, SO_2	[12]
NiS	Millerite	385	NiS, $NiSO_4$	[18]
		535	NiS, NiO, $NiSO_4$	[19]
$CuFeS_2$	Chalcopyrite	350	$CuFeS_2$, FeS_2, γ-$CuFeS_2$	[20]
		550	$CuFeS_2$, $Cu_{1.8}S$, M_xO_y	[21]
		500	$CuFeS_2$, Fe_3O_4, Fe_2O_3, FeS_2	[22]
ZnS	Sphalerite	527	ZnS, ZnO, $ZnSO_4$, Zn	[23]
		580	ZnS, ZnO, $ZnSO_4$	[23]

are non-stoichiometric, having excess sulphur, then decomposition into a stoichiometric sulphide and liberation of sulphur can occur. A typical example is the decomposition of chalcopyrite ($CuFeS_2$) to bornite (Cu_5FeS_4):

$$5CuFeS_2 \rightarrow Cu_5FeS_4 + 5FeS + S$$

This reaction was used to explain the endothermic drift observed in the DTA record between 375 and 390°C [20].

The TG–DTA curve for the oxidation of chalcocite (Cu_2S) is shown in Fig. 3 [24]. The first major exotherm is due to the oxidation of the sulphide, but then the reaction starts to slow down and the DTA record starts to return towards the baseline. At 510°C, the second major exotherm commences. It could be interpreted that these were two separate reactions. Investigation using techniques such as SEM and hot stage microscopy revealed that a thick oxide/sulphate layer had formed around the particle and arrested further oxidation. At 510°C, however, melting occurred through reaction between Cu_2S and $CuSO_4$, the oxide film was destroyed and further oxidation of the sulphide could take place. Hence, both exotherms were due to the same reaction. The two stage increase in mass due to the formation of $CuSO_4$ followed by the same pattern, with sulphate formation arrested before the melting reaction, followed by further suphate formation [24].

One of the additional features sometimes observed in the DTA trace is a number of sharp exotherms which precede the main exotherm. These peaks have

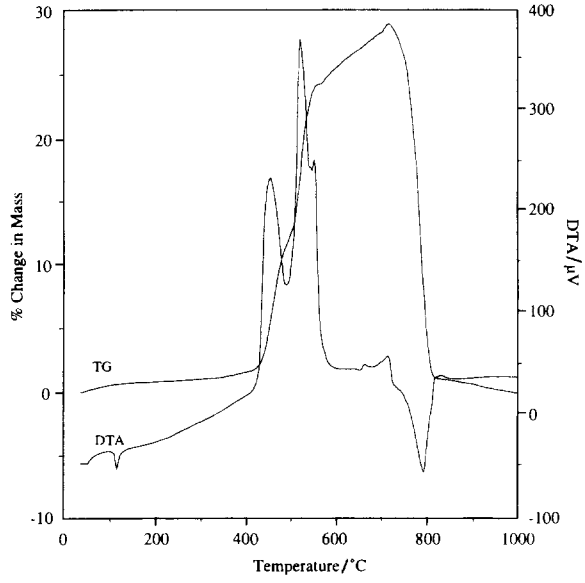

Fig. 3. TG–DTA record for the oxidation of chalcocite, Cu_2S, in air. Heating rate 10°C min^{-1}, particle size 45 to 75 μm [24].

been attributed to a number of causes, which include periodic oxygen starvation [25], preferential oxidation of some particles [26], and periodic cracking of protective oxide coatings which expose fresh sulphide for oxidation [27]. It has also been shown that this effect is particularly associated with fine particles [28]. With pyrite, for example, the number of these peaks decreased with increase in particle size, and were not apparent for a sample larger than 30 μm. The number of peaks increased with lowering of heating rate, increase in the partial pressure of oxygen and a

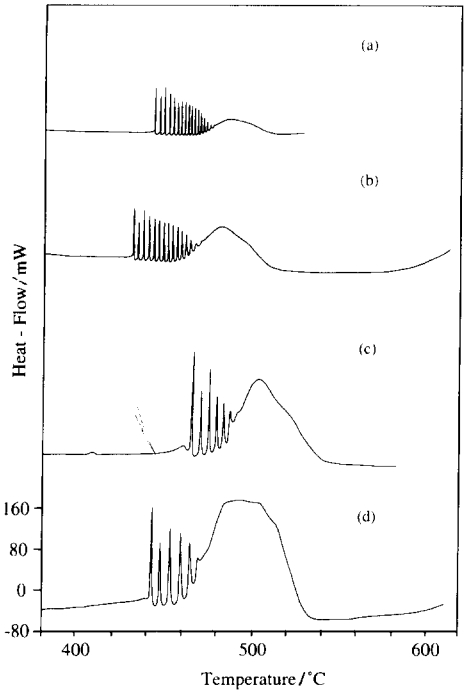

Fig. 4. The effect of heating rate on the number of multiple peaks observed during the oxidation of pyrite. Heating rates (in $°C\ min^{-1}$), (a) 1; (b) 2.5; (c) 5; and (d) 10. Oxygen atmosphere, particle size <45 μm [28].

decrease in the sample mass. The effect of changes in heating rate on the number of peaks is shown in Fig. 4, where the number of peaks reduces from 16 at a heating rate of $1°C\ min^{-1}$ to six at a heating rate of $10°C\ min^{-1}$ [28].

3.2.1.2. Formation of sulphate. The formation of sulphate can take place by two possible reactions. The first is the direct oxidation of the sulphide, as shown during the oxidation of nickel sulphide [19] and iron(II) sulphide [29]:

$$MS_{(s)} + 2O_{2(g)} \rightarrow MSO_{4(s)}$$

The second possibility is the sulphation of the oxide with sulphur trioxide:

$$MS_{(s)} + 1.5O_{2(g)} \rightarrow MO_{(s)} + SO_{2(g)}$$

$$SO_{2(g)} + 0.5O_{2(g)} \rightarrow SO_{3(g)}$$

$$MO_{(s)} + SO_{3(g)} \rightarrow MSO_{4(s)}$$

$$MS_{(s)} + 4SO_{3(g)} \rightarrow MSO_{4(s)} + 4SO_{2(g)}$$

Both $CuSO_4$ [18] and $ZnSO_4$ [30] are formed by this reaction. The formation of $CuSO_4$ is important as one of the commercial routes available for the recovery of copper from sulphide deposits. The sulphate is leached with dilute sulphuric acid followed by precipitation or electrowinning of the copper from solution [31].

The formation of sulphate is an exothermic process, but the reaction is relatively slow and takes place over a wide range of temperature. Hence, the exothermic effect is difficult to detect by DTA. Sulphate formation is associated with a weight gain by TG. This phenomenon has been observed in the oxidation of valleriite $[Cu_{0.93}Fe_{1.07}S_2].1.526[Mg_{0.68}Al_{0.32}(OH)_2]$ [32], chalcopyrite [20], nickel sulphide concentrates [33], and pentlandite [34] in the following temperature ranges: up to 650°C, 350° to 700°C, 415° to 645°C and 460° to 580°C, respectively.

The formation of sulphates can be affected by several factors, namely:

- *particle size*: sulphate formation will tend to increase as particle size decreases [35];
- *heating rate*: sulphate formation is encouraged by low heating rates [36];
- *sample holder geometry*: sulphate formation is enhanced in a shallow open sample holder, which allows good interchange between the incoming oxidising gas and the outgoing sulphur dioxide product [37];
- *sample holder material*: The formation of SO_3 is encouraged by the presence of catalytic material and, hence, the extent of sulphation increases. The catalytic influence of a platinum sample holder on sulphate formation is well known; and
- *mass size*: increasing the mass size inhibits gas diffusion, and so inhibits formation of sulphate [38].

The formation of sulphate layers can also inhibit oxygen diffusion into the unreacted core of the particle.

3.2.1.3. Decomposition of sulphates. Decomposition of sulphates take place in two stages, as expressed by the following reactions:

$$2MSO_{4(s)} \rightarrow MO.MSO_{4(s)} + SO_{3(g)}$$

and

$$MO.MSO_{4(s)} \rightarrow 2MO_{(s)} + SO_{3(g)}$$

These reactions are detectable by endotherms in the DTA trace and a weight loss in the TG curve. Such reactions have been reported for copper(II) sulphate decomposition [39], with oxysulphate being stable in the 675° to 740°C range [20], and decomposition of copper oxysulphate to copper(II) oxide above 740°C. The decomposition of $NiSO_4$ [34] occurs above 800°C. Recently, the decomposition temperatures of a number of sulphates have been listed in the ICTAC newsletter [40].

3.2.1.4. Solid–solid reactions. Solid–solid reactions can occur between the reaction products formed during the oxidation of sulphides, the most common being the reaction between unreacted sulphide and sulphate. When a particle of sulphide is oxidised, the reaction usually takes place via a shrinking core process. The oxygen attacks the outer surface, and the reaction front moves inwards. Both oxide and sulphate can be formed simultaneously, but it appears that the oxide forms an outer layer, and the sulphate exists between the oxide and the unreacted sulphide core [41]. There is obviously some overlap and the boundaries are not distinct. However, sulphur analysis by SEM, or EPMA, or Auger spectroscopy across reacted particles clearly shows that most sulphur exists in a central core; then there is a decrease in a rim near the surface and, finally, in the outermost rim it is usually difficult to detect the sulphur. Hence, it is possible for the reaction to occur between the inner core sulphide and the sulphate.

Dunn and Kelly [19] reported that a solid–solid reaction between NiS and $NiSO_4$ to form Ni_3S_2 occurred at 682°C, although the reaction did not attain completion. The rate of reaction between two solid materials is often slow, especially at low temperatures, but is facilitated if one or more of the phases melts and the reaction becomes a solid–liquid or liquid–liquid reaction. For example, interaction between synthetic copper(II) sulphide and copper(II) sulphate in an argon atmosphere was found to occur when the mixture was melted at 478°C, and a mixture of iron(II) sulphide and iron(II) sulphate melted at 490°C [18]. Reactions between oxides to form mixed metal oxides often take place at higher temperatures. For example, the reaction between CuO and Fe_2O_3 to form $CuFe_2O_4$ [20] takes place at 820 to 840°C.

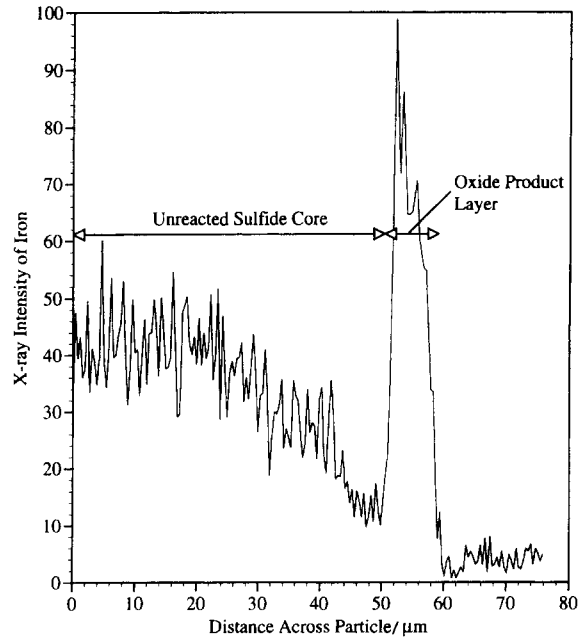

Fig. 5. Ion diffusion effects in partially oxidised samples of pentlandite heated to 650°C, particle size 90 to 125 μm [6].

3.2.1.5. Ion diffusion processes. In ternary sulphides, it is possible during the heating stage for one of the cations to preferentially diffuse towards the oxygen/oxide interface. This has been shown to occur in roasted pentlandite and violarite samples, where after a 30 min roast at 685°C the pentlandite core contained only 2.4% iron, while the outer rim was iron-rich [21]. Nickel ions have been reported to diffuse into pyrrhotite even at temperatures as low as 275°C [42]. The effect can be measured on individual particles with an SEM-energy dispersive spectrometer (EDS), and the concentration profiles plotted as a function of distance across the particle. An example is shown in Fig. 5, for a sample of pentlandite heated to 650°C in an air atmosphere [6]. An EDS scan of the unreacted particle showed that the iron–nickel distribution was uniform across each particle. As the sample is heated, iron diffuses towards the oxygen interface, and so there is iron depletion in the unreacted sulphide core, with a high concentration of iron in the oxide product layer.

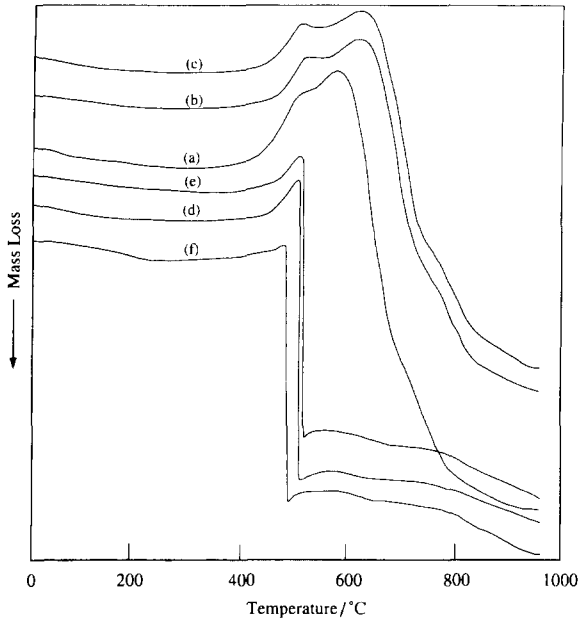

Fig. 6. TG curves of an iron–nickel sulphide concentrate showing the transition from a sequential oxidation process to an ignition reaction. Heating rates (in °C min^{-1}): (a) 1; (b) 5; (c) 10; (d) 15; (e) 30; and (f) 50. Particle size: 20 to 100 μm [33].

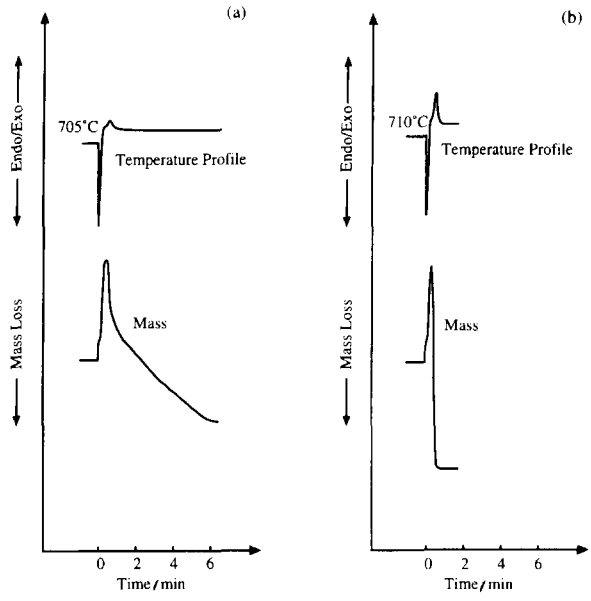

Fig. 7. Isothermal TG-curves for (a) non-ignited and (b) ignited pentlandite [6].

3.2.2. *Oxidation under vigorous oxidising conditions*

Under certain conditions, such as a high partial pressure of oxygen, a fast heating rate, and small particle size, some sulphide minerals can be persuaded to ignite. Ignition is defined as corresponding to the establishment of self sustaining combustion after the termination of heat supply from an external stimulus [43]. In TG DTA, the ignition reaction is characterised by a single high energy emission that occurs in a very narrow time span [36], or a very rapid mass loss. A typical example for the change in the TG-curve, as the reaction shifts from mild oxidising to ignition conditions, is shown in Fig. 6 [33]. The sample being heated is a nickel sulphide concentrate. At the low heating rates of 1, 5 and 10°C min^{-1} (Fig. 6a,b and c respectively), the TG curve shows the profile expected for a reaction controlled by oxygen diffusion into the particle. The mass gain is caused by the formation of sulphate, and the mass loss by the oxidation of the sulphide and the decomposition of sulphates. As the heating rate increases, the thermal events shift to higher temperature. At the faster heating rates of 15, 30 and 50°C min^{-1} (Fig. 6d, e and f), there is a striking change in the TG-curves. The formation of sulphate is still evident, but it leads to a rapid mass loss. This mass loss occurred at increasingly lower temperatures as the heating rate increased, which is the opposite trend to what might be expected. The difference in onset temperature between these mass losses and those observed at heating rates of 10°C min^{-1} or below was up to 170°C. The reaction profiles obtained under the more vigorous conditions are typical of an ignition reaction.

A TG method, which has been described as an isothermal method, was used to study the ignition reactions of iron–nickel sulphides [36]. The process involves preheating the furnace to some set temperature, and then raising the furnace around the sample. Oxygen was used as an oxidising gas. With no significant reaction evident (see Fig. 7a), the furnace was lowered, a new sample inserted, then the furnace temperature was increased and the process was repeated. This process was repeated until the next temperature increment results in a very rapid mass loss in the sample (see Fig. 7b). The sample was observed to reach red heat, and was obviously at a higher temperature than the furnace as the temperature record was distorted from the set isothermal temperature. The

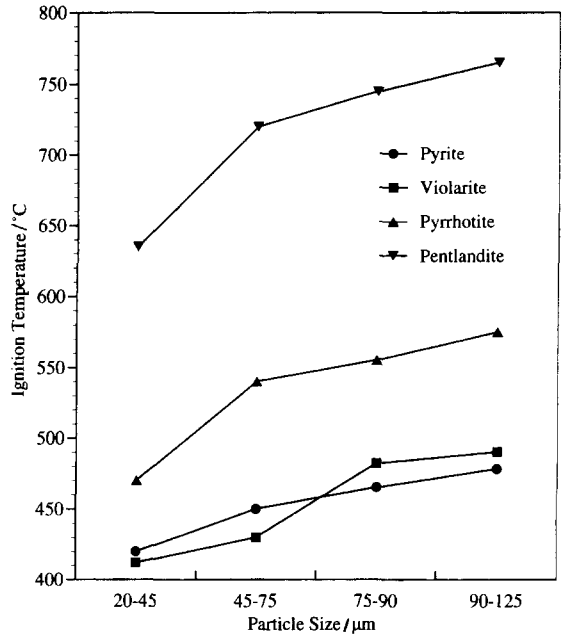

Fig. 8. Plot of ignition temperature vs. particle size for mineral sulphides [7].

temperature at which the first major reaction occurred is defined as the ignition temperature.

Using the isothermal TG technique, it was possible to compare the ignition temperatures of sulphides. The order of decreasing reactivity of four sulphides, commonly found in Western Australia,was: violarite ($FeNi_2S_4$)>pyrite (FeS_2)>pyrrhotite (FeS)>pentlandite ($(Fe,Ni)_9S_8$). The ignition temperatures for those minerals of similar particle size (45 to 75 μm) were 435°, 455°, 545° and 725°C [7]. The ignition temperature has also been found to be affected by the stoichiometry of the sulphide [8]. The ignition temperatures of pyrrhotite of particle size 45 to 63 μm and stoichiometry of $Fe_{0.83}S$, $Fe_{0.88}S$, $Fe_{0.92}S$, $Fe_{0.96}S$ and $Fe_{1.00}S$ were: 540°, 640°, 670°, 690° and 720°C, respectively. Thus, the less stoichiometric the compound, the lower the ignition temperature.

The effect of particle size on the ignition temperature of the above-mentioned sulphides was assessed by the TG method. The results are presented in Fig. 8 [7]. The smaller the particle size, the lower the ignition temperature. These results have practical importance, because the mineralogical composition of the nickel sulphide deposits can vary considerably. If the concentrate feed to the smelter consists primarily of pyrite and violarite, then flash smelting will be a facile process. If the concentrate consists of pyrrhotite and pentlandite, then higher temperatures will be required to achieve ignition. The effect of the different activity can be considerably alleviated by grinding the pyrrhotite and pentlandite concentrates to smaller sizes, which has a significant effect on the ignition temperature of these two minerals. For a number of years now, the feedstock to the flash smelter has had to meet particle size specifications, which has produced an estimated $2 million per annum saving in fuel costs [44].

Laboratory studies of this nature cannot be extrapolated directly to industrial plants, because the heat and mass transfer effects are very different between an industrial smelter and TG apparatus. What the laboratory studies enable is the determination of the effect of a variety of parameters under well controlled conditions on the ignition tendencies of sulphides, so that the parameters can be arranged in order of importance. These studies then need to be scaled up to pilot plant level, which more reliably mimics industrial plant, and the effect of the important parameters quantified. This is a very cost effective way of culling out unimportant parameters, since experimentation involving pilot scale facilities is obviously expensive. The results of the pilot scale studies have been reported elsewhere [45–47]. What has been very rewarding is that the operation of the flash smelter has changed over the years in the light of our findings.

4. Oxidation of pyrite

In order to illustrate some of the comments made earlier about the need to recognise the importance of experimental variables on the thermal analysis record, the oxidation of pyrite will be discussed as a case study. Various reaction schemes have been proposed, as indicated in Fig. 9.

Figs. 10 and 11 show the different types of DTA curves that have been reported in the literature for the oxidation of pyrite. Fig. 10(a) is an example of an experiment which shows a very broad exothermic peak in the 330° to 630°C range, with very poor resolution of any structure in the profile [50]. Pyrite is an example of a compound with a reaction rate very much in the range of the usual thermal analysis

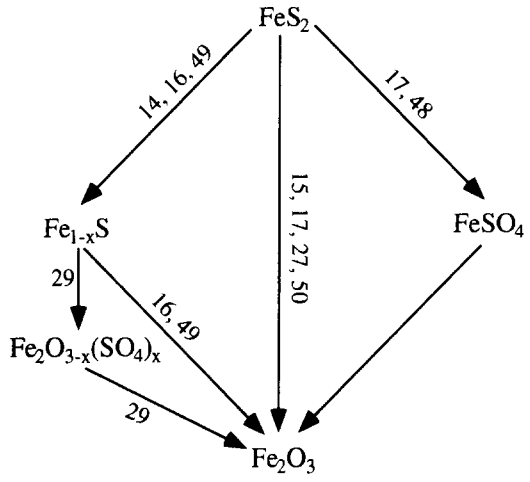

Fig. 9. Reaction schemes proposed for the oxidation of pyrite (Refs. [14–17,27,29,48–50] are indicated as numbers).

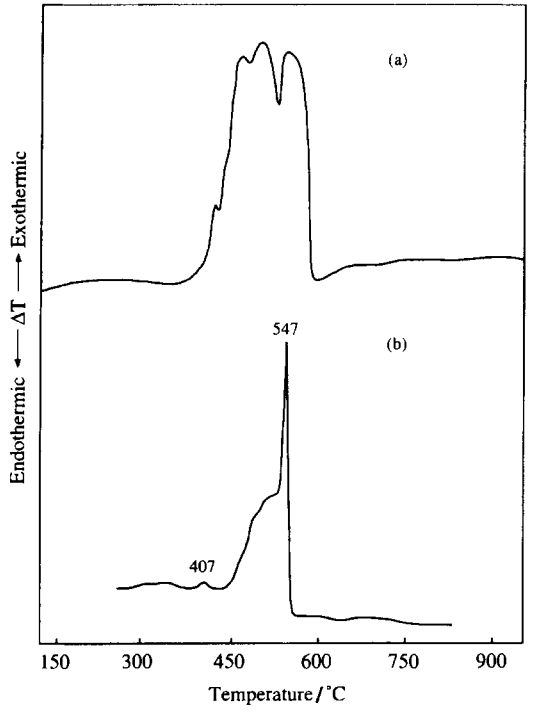

Fig. 10. DTA profiles for the oxidation of pyrite under different reaction conditions [50]: (a) 10°C min^{-1}, 21 mg sample; and (b) 4.1 mg sample diluted with Al_2O_3.

conditions. Hence, at these heating rates what is being measured is the amount of time that it takes to oxidise the pyrite. If the sample mass is increased then the

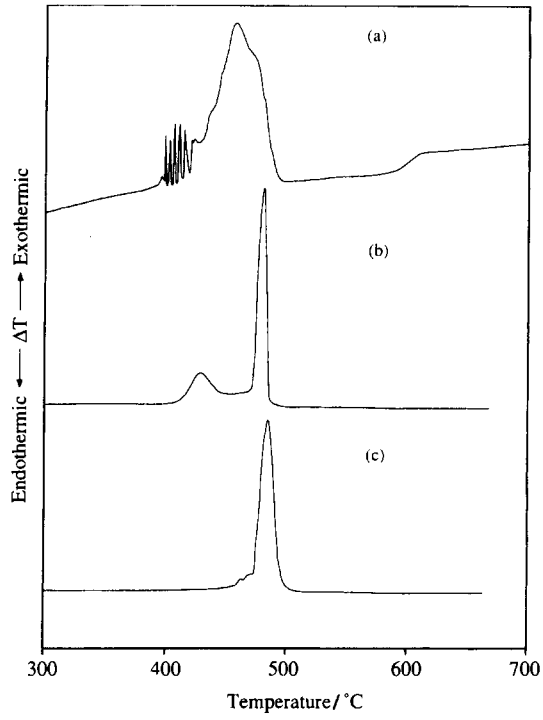

Fig. 11. DTA profiles showing the effect of heating rate, particle size and atmosphere on the oxidation of pyrite [35,51]. (a) heating rate 2.5°C min^{-1}, particle size <45 μm, DTA sensitivity 50 μV; (b) heating rate 20°C min^{-1}, particle size 90 to 125 μm, DTA sensitivity 500 μV; and (c) heating rate 40°C min^{-1}, particle size <45 μm DTA sensitivity 50 μV.

reaction takes place over an even longer time period, and so the exothermic peak broadens even further, sometimes over a 400°C range. Earnest [50] recognised this problem, and diluted the sample with alumina to produce the DTA profile shown in Fig. 10(b). This is clearly over a much narrower temperate range, with the main peak taking place between 450 to 570°C. Some resolution of thermal events is observed, with a small peak at a peak temperature of 407°C and a broad exotherm preceding a sharp exotherm with a peak temperature at 547°C.

We have made similar studies, to produce the DTA profiles shown in Fig. 11(a–c) [35,51]. The DTA record of 2 mg of a < 45 μm sample of pyrite heated in an air atmosphere and at a rate of 2.5°C min^{-1} is shown in Fig. 11(a). Several thermal events are apparent. Quantitative XRD showed that the group of sharp exotherms in the DTA record between 400 and 430°C produced < 5% Fe_2O_3. Beyond this there is a major

exotherm between 430 to 500°C. Up to 470°C 47% Fe_2O_3, and up to 505°C 65% Fe_2O_3 was produced. Hence, up to 500°C, the exotherms are associated with the direct oxidation of pyrite to form Fe_2O_3. Sulphation of some of the oxide occurs simultaneously. Beyond 550°C, the endothermic peak and mass loss (not shown) is attributed to the decomposition of the iron sulphate phase with the formation of more Fe_2O_3. SEM examination indicated that the oxidation occurred according to the classical shrinking core model in which the rate of reaction is controlled by oxygen diffusion through product coatings. If sufficient time is allowed, that is the heating rate is slow, the particles will be completely oxidised by this mechanism.

The second DTA record is of 2 mg of a 90 to 120 μm sample of pyrite heated in an air atmosphere at a rate of 20°C min^{-1} (Fig. 11b). Only two exothermic effects are evident, between 450° and 505°C, and 530° and 560°C. Quantitative XRD has shown the presence of 11% Fe_2O_3 at 453°C, 75% at 520°C, and 90% at 550°C. The micrographs produced by SEM have shown that the large particles heated to 510°C had a thick well-defined rim of oxide around a core of unreacted pyrite. Above 510°C, the character of the particles had changed; the inner core now had a very porous structure, indicative of gas evolution.

The reaction sequence for the larger particles at the faster heating rate proceeds by two different mechanisms. Up to 500°C the reaction is controlled by oxygen diffusion, and the first exothermic peak is due to the direct oxidation of pyrite to Fe_2O_3. Once the oxide rim is formed the rate of oxygen diffusion slows rapidly, and the faster heating rate combined with the larger particles ensures that even at 510°C the reaction is nowhere near completion. Beyond this temperature the decomposition of pyrite begins, and sulphur vapour is evolved. The rate of reaction is now controlled by sulphur diffusion outwards rather than oxygen diffusion inwards, and no further oxidation is evident until all the sulphur has been evolved. The sulphur burns near the surface of the particle, causing the sharp major exotherm. The resulting pyrrhotite has a very porous structure, and so oxygen diffusion into the particle to oxidise the pyrrhotite to hematite is fast and also contributes to the intensity of the exotherm. The oxidation reaction is complete by 550°C, some 45°C higher than for the small particles.

The equations relevant to these reactions are:

$$FeS_2 \rightarrow FeS + S_{(g)}$$

$$2FeS + 3.5O_2 \rightarrow Fe_2O_3 + 2SO_2$$

The final DTA trace (Fig. 11c) is for 2 mg of a < 45 μm sample of pyrite heated in oxygen at 40°C min^{-1}. This shows only one intense exothermic peak, completed at just above 500°C. There is no evidence of any second endotherm or mass loss which would indicate the decomposition of iron sulphate. XRD data on a sample, heated to just beyond the exotherm, revealed that only Fe_2O_3 was present. The SEM results indicated a porous structure typical of a reaction involving gas evolution. This sample appeared to have ignited. At fast heating rates, the heat evolved through oxidation of the surface of a pyrite particle is adsorbed by the particle rather than by the surrounding environment. The temperature of the particle is raised above the furnace temperature. If the particle temperature exceeds the decomposition temperature of pyrite then sulphur will be evolved, which oxidises rapidly in the gas phase and causes further particle heating. The reaction is self- sustaining, and complete by 500°C. Since, there was no evidence of any sulphate in the product heated at just above the exotherm, the particles had reached a high temperature enough to decompose any sulphate formed.

The DTA records obtained under the three sets of experimental conditions have been explained by three different reaction mechanisms. These explanations could only have been reached by the use of complementary characterisation techniques to assist with the interpretation of the DTA curves. The good news is that all the reports in the literature are, in fact, correct. What has not been obvious is that the schemes proposed have been true only for the set of conditions used in that particular thermal experiment. What we have provided here is a more general explanation which accounts for all the sets of conditions.

5. Conclusions

Thermal methods of analysis such as DTA and TG provide a powerful methodology for the study of sulphide minerals. When coupled with

characterisation techniques such as XRD, SEM, and FTIR, the reaction sequence can be established unambiguously. However, the thermal behaviour of sulphides can vary significantly with change in the experimental variables. The particle size, heating rate, and atmosphere are particularly important, and changes in these can produce changes in the mechanism of reaction. Hence, studies on sulphides should be conducted under a variety of experimental conditions in order to establish the conditions under which particular mechanisms prevail. In other words, carrying out experiments under one set of conditions will provide a reaction sequence only for that set of conditions, and may not be capable of extrapolation to other conditions.

The data obtained under well controlled conditions can be used to examine the importance of various experimental parameters on the reactivity and rate of reaction of the sulphides. This information can be used as a guide to define pilot plant studies, so that important parameters are investigated thoroughly while unimportant parameters are largely ignored. Thus, thermal methods of analysis can significantly reduce the costs associated with pilot plant studies.

It has been demonstrated that the transfer of the knowledge gained from thermal methods of analysis to pilot plant, and subsequently to an industrial plant, has produced significant savings in plant operations.

Acknowledgements

I would like to acknowledge the Minerals and Energy Research Institute of Western Australia, the Western Mining Corporation's Kalgoorlie Nickel Smelter, and more recently the A.J. Parker Cooperative Research Centre for Hydrometallurgy, for funding to carry out some of the above work. A special vote of thanks goes to the various graduate students who have contributed to the research programs, namely Drs. Mackey, De, Ginting, and Chamberlain, Messrs. C.E. Kelly and G. Nguyen, Mrs. V. Howes and to my colleague Mr. I. Sills.

References

[1] P.J. Haynes, Thermal Methods of Analysis, Blackie Academic and Professional, London, UK (1995) Chap. 1.
[2] J.G. Dunn and J.H. Sharp, Thermogravimetry, in J.D. Winefordner (Ed.), Part 1, Treatise on Analytical Chemistry, Vol. 13, Wiley, New York (1993) pp. 127–266.
[3] J.G. Dunn, W. Gong and D. Shi, Thermochim. Acta, 208 (1992) 293–303.
[4] J.E.H. Roseboom, Econ. Geology, 61 (1966) 641–671.
[5] I.D. Shah and S.E. Khalafalla, Metall. Trans., 2 (1971) 606–608.
[6] A.C. Chamberlain, The effect of stoichiometry on the thermal properties of violarite and pentlandite, Ph.D thesis, Curtin University, Perth, Australia (1997).
[7] J.G. Dunn and L.C. Mackey, J. Therm. Anal., 37 (1991) 2143–2164.
[8] J.G. Dunn and A.C. Chamberlain, J. Therm. Anal., 37 (1991) 1329–1346.
[9] I.E. Gurbunova, V.M. Grigor'yeva, L.S. Tsemekhman, L.P. Ivanchenco and N.N. Shinshkin, Russian Met. (English translation), 6 (1978) 28–32.
[10] H.H. Kellogg and S.K. Basu, Trans. Met. Soc. AIME, 218 (1960) 70–81.
[11] O.C. Kopp and P.F. Kerr, Amer. Mineralogist, 43 (1958) 1079–1097.
[12] F.R.A. Jorgensen and F.J. Moyle, J. Therm. Anal., 25 (1982) 473–485.
[13] F.R.A. Jorgensen and F.J. Moyle, J. Therm. Anal., 31 (1986) 145–156.
[14] F. Paulik, J. Paulik and M. Arnold, J. Therm. Anal., 25 (1982) 313–325.
[15] J.R. Schorr and J.O. Everhart, J. Amer. Ceram. Soc., 52(7) (1969) 351.
[16] F.R.A. Jorgensen and F.J. Moyle, J. Therm. Anal., 29 (1984) 13–17.
[17] A.C. Banerjee, Indian J. Chem., 14A(November) (1976) 845–850.
[18] E.M. Kurian and R.V. Tamhankar, Trans. Indian Inst. Metals, June 1971, pp. 17–21.
[19] J.G. Dunn and C.E. Kelly, J. Therm. Anal., 12 (1977) 43–52.
[20] M. Aneesuddin, P.N. Char, M.R. Hussain and E.R. Saxena, J. Therm. Anal., 26 (1983) 205–216.
[21] P.G. Thornhill and L.M. Pidgeon, J. Metals, 9 (1957) 989–995.
[22] R.G. Henley, H.C. Hsio and F.R.A. Jorgensen, Advances in Sulfide Smelting, 1 (1983) 81–98.
[23] R. Dimitrov and I. Bonev, Thermochim. Acta, 106 (1986) 9–25.
[24] J.G. Dunn, A.R. Ginting and B. O'Connor, J. Therm. Anal., 41 (1994) 671–686.
[25] R.J.W. McLaughlin, Other Minerals, in: R.C. Mackenzie (Ed.), Differential Thermal Analysis of Clays, Mineralogical Society of London (1957) p. 367.
[26] E.M. Bollin, Chalcogenides, in: R.C. Mackenzie (Ed.), Differential Thermal Analysis, Vol. 1, Academic Press, New York (1970) p. 203.
[27] F.R.A. Jorgensen and F.J. Moyle, Met. Trans., 12B (1981) 769.
[28] J.G. Dunn, G.C. De and P.G. Fernandez, Thermochim. Acta, 135 (1988) 267–272.

[29] T. Kennedy and B.T. Sturman, J. Therm. Anal., 8 (1975) 329–337.
[30] F. Habashi and R. Dugdale, Met. Trans., 4 (1973) 1553–1556.
[31] A.K. Biswas and W.G Davenport, Extractive Metallurgy of Copper, Pergamon Press, Oxford (1976) pp. 16–17, 61–62, 113–116, 160.
[32] A.L. Iglesia, M. Doval and F. Lopez-Aguayo, American Miner., 62 (1977) 1030.
[33] J.G. Dunn and S.A.A. Jayaweera, Thermochim. Acta, 61 (1983) 313–317.
[34] J.G. Dunn and C.E. Kelly, J. Therm. Anal., 18 (1980) 147–154.
[35] J.G. Dunn, G.C. De and B.H. O'Connor, J. Therm. Anal., 145 (1989) 115–130.
[36] J.G. Dunn, S.A. Jayaweera and S.G. Davies, Proc. Austral. Inst. Min. Met., 290 (1985) 75–82.
[37] G. Hakvoort, Thermochim. Acta, 233 (1994) 63–73.
[38] G.C. De, A study of the oxidation of pyrite using thermal analysis techniques. Master Thesis, Curtin University of Technology, Perth, Australia (1987).
[39] T.R. Ingraham, Trans. Met. Soc. AIME, 233 (1965) 359–363.
[40] V. Pelovski, ICTAC News, 2 (1994) 95–103.
[41] C. Jones, S. Count, R. Smart and T. White, App. Surface Chem., 55 (1992) 65–85.
[42] W.E. Ewers, Proc. Austral. Inst. Min. Met., 241 (1972) 19.
[43] V.N. Vilyunov and V.E. Zarko, Ignition of Solids, Elsevier, Amsterdam (1989) p. 320.
[44] C.W. Hastie, D.R.T. Hall, C.A. Hohnen and J.M. Limerick, in Symposium on Extractive Metallurgy, Austral., Inst. Min. Met., Melbourne, Victoria, Australia (1984) pp. 309–316.
[45] J.G. Dunn, L.C. Mackey, I.R. Stevenson and T.N. Smith, Trans. Inst. Min. Met., Section C, 100 (1991) 105–109.
[46] J.G. Dunn, L.C. Mackey, I.R. Stevenson and T.N. Smith, Trans. Inst. Min. Met., Section C, 101 (1992) 87–90.
[47] J.G. Dunn, L.C. Mackey, T.N. Smith and I.R. Stevenson, Trans. IMM, Section C, 102 (1993) 75–82.
[48] V.A. Luganov and V.I. Shablin, Canad. Met. Quart., 21(2) (1982) 157.
[49] R.A. Schoenlaub, J. Am. Chem. Soc., 52(1) (1969) 40.
[50] C.M. Earnest, Thermochim. Acta, 75 (1984) 219–232.
[51] J.G. Dunn, G.C. De and B.H. O'Connor, Thermochim. Acta, 155 (1989) 135–149.